Application of the Strongly Coupled-Mode Theory to Integrated Optical Devices

SHUN-LIEN CHUANG, MEMBER, IEEE

Abstract—**A theory for strongly coupled waveguides is discussed and applied to two- and three-waveguide couplers and optical wavelength filters. This theory makes use of an exact analytical relation governing the coupling coefficients and the overlap integrals. It removes almost all of the constraints imposed by a simpler and approximate coupled-mode theory by Marcatili. It also satisfies the energy conservation and the reciprocity theorem self-consistently. We show very good numerical results with the overlap integral as large as 49 percent. The applications to electrooptical modulators, power dividers, power transfer devices, and optical filters are all presented with numerical results.**

I. Introduction

THE applications of the coupled-mode theory in integrated optical devices, such as waveguide couplers [1]–[3], laser arrays [4], [5], and optical filters [6]–[8], have been well known. However, theoretical improvements for strongly coupled waveguides have only been attempted very recently [9]–[14]. A simple and approximate version of coupled-mode equations for parallel dielectric waveguides has also been presented by Marcatili [15] to account for the asymmetric properties of waveguides using a newly found relation between the coupling coefficients and the overlap integral of two-coupled waveguides. A few conditions are assumed in that paper:

1) A scalar formulation of the fields is considered.

2) The refractive index perturbation is very small such that second-order terms can be ignored.

$$n^2 = n_0^2\left[1 + \Delta_a(x, y) + \Delta_b(x, y)\right]^2 \simeq n_0^2\left[1 + 2\Delta_a(x, y) + 2\Delta_b(x, y)\right] \quad (1)$$

Thus the new relation between the two coupling coefficients in [15] is only approximate.

3) The overlap integral c is assumed to be small (weakly coupling) and is not included in the coupled-mode equations because the coupled-mode equations in [15] are almost the same as those for the conventional theory [2] without including the overlap integrals in the four coupling parameters, γ_a, γ_b, K_{ab}, and K_{ba}.

In this paper, we apply the theory developed in [9]–[14] and show that all the above conditions are not required. It is shown that an exact analytical relation governing the coupling coefficients, the overlap integrals, and the propagation constants derived in [13] using a generalized reciprocity theorem can be combined with the formulation of Marcatili and will give very good numerical results even for strongly coupled waveguides. It has been pointed out in [9] that the four parameters γ_a, γ_b, K_{ab} and K_{ba} should include the overlap integrals to obtain correct propagation constants of the supermodes. Since only β_a, β_b of individual waveguides and K_{ab}, K_{ba} of the conventional coupling coefficients are used in the coupled-mode equations in [15], that theory will not yield accurate numerical results and may violate energy conservation significantly [9], [13] unless the overlap integral $c \ll 1$, which is assumed in [15].

In Section II, we briefly review the strongly coupled-mode equations derived in [9]–[11], [13], and [14], their orthogonality relation, and an exact relation between the coupling coefficients K_{ab} and K_{ba}. We also show that this exact relation can also be derived from power conservation or reciprocity relation for a lossless medium. In Section III, we consider the two-coupled waveguides combining the strong coupling of mode equations and the formulation of [15], and illustrate the electrooptic effect. We then study the three waveguide couplers as power transfer devices and power dividers. Previous studies in [16] and [17] assume all three guides have the same refractive indexes, and a direct numerical approach for the multilayered structure is taken. In Section IV, the crosstalk problems for both two- and three-coupled waveguides are investigated. Numerical results are presented and compared with those in [18] and [19]. In Section V, the application of the coupled-mode theory to the optical wavelength filters is studied and the theoretical results are compared with the experimental results in [8]. Finally, we give conclusions in Section VI.

II. Theory of Strongly Coupled Waveguides

Three very similar formulations of strongly coupled waveguides have been presented in [9], [12], [13]. The formulation by Haus *et al.* [12] is limited to the lossless system and has a small difference in the z-component of the electric field for the trial functions in the variational approach. The formulation of Hardy–Streifer [9] does not satisfy energy conservation and the reciprocity theorem and still contains a small error, while the theory of [13] (which was derived in a much simpler way) satisfies these

Manuscript received August 25, 1986; revised November 24, 1986. This work was supported in part by NASA Grant NAG1-500.

The author is with the Department of Electrical and Computer Engineering, University of Illinois at Urbana-Champaign, Urbana, IL 61801.

IEEE Log Number 8613381.

laws analytically. Independently, a reformulation of [9] has been made [20] recently and is identical to that of [13] after the modifications. The coupled-mode equation in [13], [14] and its properties are summarized below.

A. Strongly Coupled-Mode Equation

The coupled-mode equation in vector form is given [13], [14], [20] by

$$\overline{\boldsymbol{C}} \frac{d}{dz} \boldsymbol{a}(z) = \boldsymbol{Q}\boldsymbol{a}(z) \tag{2}$$

or

$$\frac{d}{dz} \boldsymbol{a}(z) = \boldsymbol{M}\boldsymbol{a}(z) \tag{3}$$

where

$$\boldsymbol{Q} = \overline{\boldsymbol{C}}\boldsymbol{B} + \boldsymbol{K} \tag{4}$$

$$\boldsymbol{M} = \overline{\boldsymbol{C}}^{-1}\boldsymbol{Q} = \boldsymbol{B} + \overline{\boldsymbol{C}}^{-1}\boldsymbol{K} \tag{5}$$

where the vector $\boldsymbol{a}(z)$ has each element $a_p(z)$ given by the electric field amplitude for the transverse component of the mode in waveguide p, and the matrix elements $\overline{C}_{pq}$ and K_{pq} are defined in Appendix A. The matrix $\boldsymbol{B}$ is a diagonal matrix with the diagonal elements given by β_1, β_2, $\cdots$, β_N of each individual waveguide in the absence of all other waveguides. It should be noted that 1) the two matrices $\overline{\boldsymbol{C}}$ and $\boldsymbol{Q}$ are symmetric [13], [14], [20] and that is very important to prove the orthogonality property of the supermodes, and 2) the matrix $\boldsymbol{M}$ is not necessarily symmetric in general.

B. Orthogonality of the Supermodes

The supermodes of the multiwaveguide system satisfy the orthogonality relation [14] for symmetric matrices $\overline{\boldsymbol{C}}$ and $\boldsymbol{Q}$ in (2)

$$\boldsymbol{a}^{(i)T}\overline{\boldsymbol{C}}\boldsymbol{a}^{(j)} = 0 \qquad \text{for} \qquad \gamma_i \neq \gamma_j \tag{6}$$

where $\boldsymbol{a}^{(i)}(\boldsymbol{a}^{(j)})$ is the eigenvector of the supermode with the propagation constant $\gamma_i(\gamma_j)$, and the superscript T denotes the transpose of the matrix or vector.

C. Reciprocity Condition

To satisfy the reciprocity relation, one finds that [14]

$$\overline{\boldsymbol{C}}\boldsymbol{M} = (\overline{\boldsymbol{C}}\boldsymbol{M})^T, \tag{7}$$

i.e., the matrix $\boldsymbol{Q}$ must be symmetric which is true as derived in [14]. For two-coupled waveguides

$$\boldsymbol{M} = \begin{bmatrix} \gamma_a & K_{ab} \\ K_{ba} & \gamma_b \end{bmatrix}. \tag{8}$$

Equations (7) and (8) give

$$K_{ab} - K_{ba} = (\gamma_a - \gamma_b)\bar{c} \tag{9}$$

where $\bar{c} = \overline{C}_{12} = (C_{12} + C_{21})/2$ (see Appendix A). The above formulation is true in general for both lossy and lossless systems. If the system is lossless, one may also have a slightly different formulation as presented in [12], [14] using field quantities involving complex conjugates.

D. Power Conservation

If the multiwaveguide system is lossless, one can choose the transverse field components $\boldsymbol{E}_t$ and $\boldsymbol{H}_t$ to be real functions and find that $\boldsymbol{E}_z$ and $\boldsymbol{H}_z$ are purely imaginary and C_{pq} and K_{pq} are real [14]. The total power guided by the multiwaveguide system is

$$P(z) = \tfrac{1}{2}\,\mathrm{Re}\iint \boldsymbol{E}_t \times \boldsymbol{H}_t^* \cdot \hat{z}\,dx\,dy$$

$$= \boldsymbol{a}^+(z)\overline{\boldsymbol{C}}\boldsymbol{a}(z) \tag{10}$$

where the superscript + denotes the conjugate and transpose of the vector $\boldsymbol{a}(z)$, and one has chosen $\boldsymbol{E}_t^{(q)}$ and $\boldsymbol{H}_t^{(p)}$ to be real. Thus using the fact that $\overline{\boldsymbol{C}}$ and $\boldsymbol{Q}$ are real matrices, one finds that the condition $d\boldsymbol{P}(z)/dz = 0$ also leads to $\boldsymbol{Q} = \boldsymbol{Q}^T$ or $\boldsymbol{C}\boldsymbol{M} = (\boldsymbol{C}\boldsymbol{M})^T$, which is the same as the reciprocity condition in (7). Actually, condition (7) is very general since it is applicable to both lossy and lossless cases. A similar formulation (for a lossless medium) leads to the fact that $\boldsymbol{Q}$ is Hermitian provided one uses complex conjugate quantities with $\overline{\overline{\boldsymbol{C}}}_{pq}$ and $\tilde{\overline{\boldsymbol{C}}}_{pq}$ matrices as defined in [14]. The Hermitian matrix becomes obviously symmetric when it is real. Another derivation of the lossless condition for two-coupled waveguides is shown in Appendix B, which also leads to (9) when γ_a, γ_b, K_{ab}, K_{ba} are real.

III. Two- and Three-Coupled Waveguides and Improvement of Marcatili's Theory

In this section, we present a combination of the vector formulation for strongly coupled waveguides and Marcatili's theory which assumes two weakly coupled waveguides. We also discuss the applications to three coupled waveguides used as either power transfer devices transferring power from one outer guide to another or as power dividers. The electrooptic effects when these devices are used as modulators are discussed.

A. Two Coupled Waveguides

1) Improvement of Marcatili's Formulation: We start with the coupled-mode equations

$$\frac{da}{dz} = i\gamma_a a + iK_{ab}b \tag{11a}$$

$$\frac{db}{dz} = i\gamma_b b + iK_{ba}b \tag{11b}$$

where

$$\gamma_a = \beta_1 + (K_{11} - \overline{C}_{12}K_{21})/(1 - \overline{C}_{12}^2) \tag{12a}$$

$$\gamma_b = \beta_2 + (K_{22} - \overline{C}_{12}K_{12})/(1 - \overline{C}_{12}^2) \tag{12b}$$

$$K_{ab} = (K_{12} - K_{22}\overline{C}_{12})/(1 - \overline{C}_{12}^2) \tag{12c}$$

$$K_{ba} = (K_{21} - K_{11}\overline{C}_{12})/(1 - \overline{C}_{12}^2) \tag{12d}$$

where the subscript 1 refers to waveguide a or 1, and 2 refers to waveguide b or 2, whichever is convenient.

One notes that in the theory of Marcatili [15], 1) $\overline{C}_{12}$ is assumed to be zero in the above four parameters, 2) K_{11} and K_{22} are ignored, and 3) K_{12} and K_{21} are defined only for scalar fields (pure TE case). Thus, that formulation is almost the same as that for the conventional theory [2] and will lead to significant errors if $\overline{C}_{12}$ becomes larger than, say, 10 percent (C_{11} and C_{22} are normalized to be 1) [9], [13]. One notes that an exact relation holds between the conventional coupling coefficients [13]

$$K_{12} - K_{21} = (\beta_1 - \beta_2)\frac{C_{12} + C_{21}}{2} \tag{13}$$

while a similar relation found in [15] is only approximate since the derivations there have assumed the refractive index variation $\Delta_a(x, y)$ and $\Delta_b(x, y) << 1$ (which is a good practical approximation). Using this relation, one can show that the following relation is true using (12), (13) and $\overline{c} = \overline{C}_{12} = \overline{C}_{21}$:

$$K_{ab} - K_{ba} = (\gamma_a - \gamma_b)\overline{c} \tag{14}$$

which is precisely the reciprocity condition, and it is the same as the power conservation condition for a lossless case (Appendix B). We define the asynchronism factor [15] in terms of the more correct parameters γ_a, γ_b, K_{ab}, and K_{ba} in (12a)–(12d).

$$\delta = \frac{\gamma_b - \gamma_a}{2\sqrt{K_{ab}K_{ba}}}. \tag{15}$$

Given the initial excitation at $z = 0$ of a two-coupled waveguide, $a(0) = 1$, $b(0) = 0$, we obtain [9], [13]

$$a(l) = \left[\cos \psi l - i\frac{\Delta}{\psi}\sin \psi l\right] e^{i\phi l} \tag{16a}$$

$$b(l) = \frac{iK_{ba}}{\psi}\sin \psi l\, e^{i\phi l} \tag{16b}$$

where

$$\phi = \frac{\gamma_b + \gamma_a}{2} \tag{17a}$$

$$\psi = \sqrt{\Delta^2 + K_{ab}K_{ba}} \tag{17b}$$

$$\Delta = \frac{\gamma_b - \gamma_a}{2}. \tag{17c}$$

It is easy to show also

$$\delta = \frac{1}{2\overline{c}}\left[\sqrt{\frac{K_{ba}}{K_{ab}}} - \sqrt{\frac{K_{ab}}{K_{ba}}}\right] \tag{18}$$

or

$$\sqrt{\frac{K_{ba}}{K_{ab}}} = \overline{c}\delta + \sqrt{1 + \overline{c}\delta} = e^{\sinh^{-1}\overline{c}\delta}. \tag{19}$$

The solutions (16a) and (16b) can be written as

$$a(l) = \left\{\cos\left[\sqrt{K_{ab}K_{ba}}l(1 + \delta^2)^{1/2}\right] - i\frac{\delta}{(1 + \delta^2)^{1/2}} \cdot \sin\left[\sqrt{K_{ab}K_{ba}}l(1 + \delta^2)^{1/2}\right]\right\} e^{i\phi l} \tag{20a}$$

$$b(l) = i\frac{e^{\sinh^{-1}\overline{c}\delta}}{\sqrt{1 + \delta^2}}\sin\left[\sqrt{K_{ab}K_{ba}}l(1 + \delta^2)^{1/2}\right] e^{i\phi l}. \tag{20b}$$

The output power P_a in waveguide a when waveguide b terminates at $z = l$ is obtained using

$$\boldsymbol{E}_t(x, y, z = l) \simeq a(l)\,\boldsymbol{E}_t^{(a)}(x, y) + b(l)\,\boldsymbol{E}_t^{(b)}(x, y) \tag{21a}$$

$$= \sum_{n=1}^{\infty} u_n^{(a)}\,\boldsymbol{E}_t^{(a)n}(x, y) \tag{21b}$$

$$\boldsymbol{H}_t(x, y, z = l) \simeq a(l)\,\boldsymbol{H}_t^{(a)}(x, y) + b(l)\,\boldsymbol{H}_t^{(b)}(x, y) \tag{22a}$$

$$= \sum_{n=1}^{\infty} v_n^{(a)}\,\boldsymbol{H}_t^{(a)n}(x, y) \tag{22b}$$

where the expansion in (21a) or (22a) is in terms of individual waveguide modes and in (21b) or (22b) is in terms of all the guided and radiation modes of waveguide a alone since they form a complete set [9]. Multiplying (21) by $\boldsymbol{H}_t^{(a)}$ and integrating over the cross section, one obtains

$$u_1^{(a)} = a(l) + C_{12}b(l). \tag{23}$$

Similarly, one finds

$$v_1^{(a)} = a(l) + C_{21}b(l). \tag{24}$$

These boundary conditions at $z = 0$ and $z = l$ follow very closely those in [15]. The guided power due to the first mode β_1 in waveguide a is, thus,

$$P_a = \frac{1}{2}\,\mathrm{Re}\left[u_1^{(a)}v_1^{(a)*}\frac{1}{2}\int\int \boldsymbol{E}_t^{(a)1} \times \boldsymbol{H}_t^{(a)1} \cdot \hat{z}\, dxdy\right]$$

$$= 1 - \left(\frac{1 - C_{12}C_{21}}{1 + \delta^2}\right) e^{2\sinh^{-1}\overline{c}\delta} \cdot \sin^2\left[\sqrt{K_{ab}K_{ba}}l(1 + \delta^2)^{1/2}\right] \tag{25}$$

using (20), (23), and (24). A similar procedure for the output power in waveguide b when waveguide a is terminated at $z = l$ leads to

$$P_b = \mathrm{Re}\left[(C_{21}a + b)(C_{12}^*a^* + b^*)\right]$$

$$= C_{12}C_{21} + \frac{1 - C_{12}C_{21}}{1 + \delta^2}\sin^2\left(\sqrt{K_{ab}K_{ba}}l(1 + \delta^2)^{1/2}\right). \tag{26}$$

These results are very similar to those in [15] except the

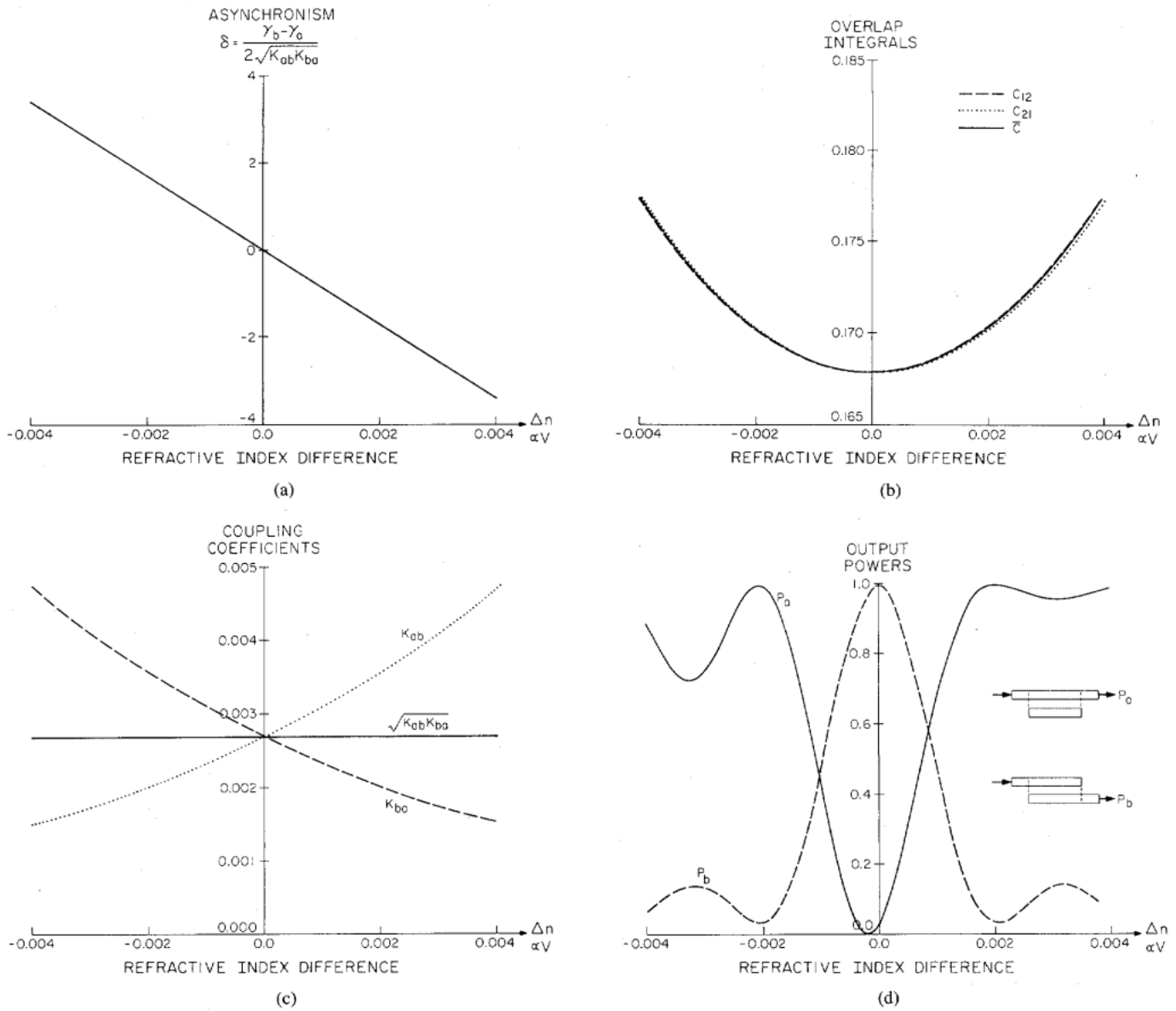

Fig. 1. (a) The asynchronism δ is plotted versus the refractive index difference of two-coupled waveguides, $\Delta n = n_a - n_b$, which is proportional to the applied voltage V. (b) The overlap integrals C_{12} (dashed line), C_{21} (dotted line) and $\bar{C} = (C_{12} + C_{21})/2$ (solid line) are shown. (c) The coupling coefficients K_{ab}, K_{ba} and $\sqrt{K_{ab}K_{ab}}$ are plotted versus Δn. (d) The output powers in guide a, P_a (solid curve), and in guide b, P_b (dashed curve), are plotted versus Δn. The parameters are $d_a = d_b = 2$ μm, waveguide edge-to-edge separation $t = 1.9$ μm, wavelength $\lambda = 1.06$ μm. $n_a = 2.2 + \Delta n/2$, $n_b = 2.2 - \Delta n/2$. The outside refractive index $n_0 = 2.19$. The coupler length $l = 0.5811$ mm.

parameters are defined in terms of the more accurate parameters γ_a, γ_b, K_{ab}, and K_{ba}.

2) Numerical Results for Two Strongly Coupled Waveguides: In Fig. 1(a)–(d), we show numerical results for two coupled Ti-diffused $LiNbO_3$ channel waveguides modeled as two-coupled slab waveguides (which is possible using the effective index method [11]) with the refractive index in waveguide a, $n_a = 2.2 + \Delta n/2$, the effective refractive index in waveguide b, $n_b = 2.2 - \Delta n/2$, where the refractive index difference

$$\Delta n = n_a - n_b \tag{27}$$

is proportional to the externally applied voltage V across the two waveguides. The refractive index outside the two waveguides is assumed to be constant, $n_0 = 2.19$. The waveguide dimensions are $d_a = d_b = 2$ μm; the edge-to-edge separation $t = 1.9$ μm. The wavelength λ is 1.06 μm. In Fig. 1(a), the asynchronism δ is plotted versus the refractive index difference. We see clearly that $|\delta|$ is linearly proportional to $|\Delta n|$. The overlap integrals C_{12} (dashed line) and C_{21} (dotted line) with their arithmetic average $\bar{c}$ (solid line) are shown in Fig. 1(b), where they vary between 0.168 at $\Delta n = 0$ to around 0.178 which do not satisfy the condition in [15] for weak coupling ($c \lesssim$

0.1). The numerical results for the propagation constants are calculated with more than 7 digits of accuracy, and the energy conservation law [14] is also checked to be valid with errors always less than 10^{-7}. (In [14], two energy conservation violation factors have been defined and are used to check the numerical accuracy of the results.) Fig. 1(b) differs slightly from the qualitative drawing of [15] with a range of variation in the overlap integrals around $(0.178-0.168)/0.168 \simeq 6.0$ percent. The coupling coefficients K_{ab}, K_{ba}, and $\sqrt{K_{ab}K_{ba}}$ are shown in Fig. 1(c), which agree well with the qualitative results of [15]. The output powers P_a (solid curve) and P_b (dashed curve) are shown in Fig. 1(c). They do agree very well with the qualitative drawing of [15]. One notes that the minimum of P_a does not occur right at $\Delta n = 0$ (where $P_b = 1.0$) due to the crosstalk problems which are discussed in Section IV. The power P_a actually goes to almost zero ($P_a = 0.00051 = 33$ dB) at $\Delta n \cong -0.0002$, where P_b reduces to 0.9723. The asymmetry of P_a and the symmetric properties of P_b versus Δn or the applied voltage agree very well with what has been presented in [15]. However, our numerical approach provides very good numerical results even for the strongly coupled case with $\bar{c} > 0.1$, while the theory of [15], although taking into account the asymmetry properties of coupled waveguides, is limited to weak coupling cases.

B. Three-Coupled Waveguides

Let us consider a symmetric case for which the two outer waveguides are identical. Solutions for this case have been obtained in [10], [11], and [14] and will not be derived here.

1) Power Transfer Devices: When used as power transfer devices, the three-coupled waveguides are assumed to have an initial excitation at $z = 0$

$$\boldsymbol{a}(0) = \begin{bmatrix} 1 \\ 0 \\ 0 \end{bmatrix} \tag{28}$$

and the input power P_{IN} is easily found to be 1.

The solutions at position z are found to be [10], [11]

$$a_1(z) = \frac{1}{2}\left\{\left(\cos\frac{\psi z}{2} - i\frac{2m_{22}-\phi}{\psi}\sin\frac{\psi z}{2}\right)e^{i(\phi/2)z} + e^{i\gamma_2 z}\right\} \tag{29a}$$

$$a_2(z) = i\frac{2m_{21}}{\psi}\sin\left(\frac{\psi z}{2}\right)e^{i(\phi/2)z} \tag{29b}$$

and

$$a_3(z) = \frac{1}{2}\left\{\left(\cos\frac{\psi z}{2} - i\frac{2m_{22}-\phi}{\psi}\sin\frac{\psi z}{2}\right)e^{i(\phi/2)z} - e^{i\gamma_2 z}\right\} \tag{29c}$$

where

$$\psi = \sqrt{(m_{11} + m_{13} - m_{22})^2 + 8m_{12}m_{21}} \tag{30a}$$

$$\phi = m_{11} + m_{13} + m_{22} \tag{30b}$$

and the three propagation constants of the supermodes are

$$\gamma_1 = \frac{\phi + \psi}{2} \tag{31a}$$

$$\gamma_2 = m_{11} - m_{13} \tag{31b}$$

$$\gamma_3 = \frac{\phi - \psi}{2} \tag{31c}$$

where the matrix elements m_{ij} have been derived in [10], [11], and [14].

The output power in waveguide 1 at $z = l$, where waveguides 2 and 3 terminate, is

$$P_{\text{out},1} = \text{Re}\left\{[a_1(l) + C_{12}a_2(l) + C_{13}a_3(l)] \cdot [a_1(l) + C_{21}a_2(l) + C_{31}a_3(l)]^*\right\} \tag{32}$$

following a similar procedure as in (21)–(26). The output power at waveguide 3 when waveguides 1 and 2 terminate at $z = l$ is

$$P_{\text{out},3} = \text{Re}\left\{[C_{31}a_1(l) + C_{32}a_2(l) + a_3(l] \cdot [C_{13}a_1(l) + C_{23}a_2(l) + a_3(l)]^*\right\}. \tag{33}$$

When applying (32) and (33) to a power transfer device, one may need to assume $|C_{13}|$ and $|C_{31}|$ are small since waveguides 1 and 3 are not terminated.

2) Power Dividers: When used as power dividers, the three-coupled waveguides have an initial excitation at $z = 0$

$$\boldsymbol{a}(0) = \begin{bmatrix} 0 \\ 1 \\ 0 \end{bmatrix} \tag{34}$$

and the input power P_{IN} can be found to be 1. The solutions at position z are [10], [14]

$$a_1(z) = a_3(z) = i\frac{2m_{12}}{\psi}\sin\frac{\psi z}{2}e^{i(\phi/2)z} \tag{35a}$$

$$a_2(z) = \left[\cos\frac{\psi z}{2} + i\frac{2m_{22}-\phi}{\phi}\sin\frac{\psi z}{2}\right]e^{i(\phi/2)z}. \tag{35b}$$

One finds the output powers in waveguide 1 and 3 to be equal using (35) in (32) or (33) since the two outer guides are identical.

3) Numerical Results for Power Transfer Devices and Power Dividers: The three-coupled waveguides considered here are assumed to be symmetric with respect to the center guide. We assume the dimensions of the three waveguides to be $d_1 = d_2 = d_3 = 2$ μm. The edge-to-edge separation of two nearby waveguides $t = 1.9$ μm.

The wavelength λ is 1.06 μm. The refractive indexes are assumed to be

$$n_1 = n_3 = 2.2 + \frac{\Delta n}{2} \tag{36a}$$

$$n_2 = 2.2 - \frac{\Delta n}{2} \tag{36b}$$

where the refractive index difference between either one of the outer guides and the center guide $\Delta n = n_1 - n_2$ is proportional to the applied voltage V. We first plot the unnormalized asynchronism $2\gamma_2 - \gamma_1 - \gamma_3$ versus the refractive index difference Δn. One sees clearly at $\Delta n = 0$ the fact that all three guides are identical does not imply the synchronism condition

$$2\gamma_2 - \gamma_1 - \gamma_3 = 0 \tag{37}$$

is met. At $\Delta n = 0$, we find

$$\gamma_1 = 13.0172261$$

$$\gamma_2 = 13.0138696$$

$$\gamma_3 = 13.0094738$$

and

$$2\gamma_2 - \gamma_1 - \gamma_3 = 0.0010393.$$

Choosing the coupling length l to be fixed at $L_{C0} = 2\pi/\psi_0$ where

$$\psi_0 = (\gamma_1 - \gamma_3) \quad \text{at} \quad \Delta n = 0 \tag{38}$$

we find the output powers $P_{\text{out},1}$ (solid curve) and $P_{\text{out},3}$ (dashed curve) as shown in Fig. 2(b) when the waveguides are used as power transfer devices. Peak power transfer from guide 1 to guide 3 actually does not occur at $\Delta n = 0$ as can be seen from Fig. 2(b). This is due to the crosstalk problem when the synchronism condition is not met. It occurs actually at $2\gamma_2 - \gamma_1 - \gamma_3 = 0$, i.e., when $\Delta n \cong -0.00023$. The crosstalks are calculated in Section IV. When used as power dividers, the three-coupled waveguides are assumed to have a coupling length $l = \pi/\psi_0 = L_{C0}/2$. The output powers in guides 1 and 3 versus the refractive index difference Δn are shown in Fig. 2(c). Maximum output power does occur at $\Delta n = 0$ for the power dividers.

In Figs. 3(a) and (b), we show the output powers $P_{\text{out},1}$ and $P_{\text{out},3}$ versus the coupling distance l normalized to $L_C = 2\pi/(\gamma_1 - \gamma_3)$ for $\Delta n = 0$ ($L_C = L_{C0}$ in this case). Since the synchronism condition is not met, $P_{\text{out},1}$ does not go to zero due to the crosstalk problems. Both $P_{\text{out},1}$ and $P_{\text{out},3}$ do not show periodic behaviors for the power transfer devices that have been discussed in [10], [11], although only the magnitudes of $|a_1(l)|$, $|a_2(l)|$ or $|a_3(l)|$ instead of powers are presented there. This nonperiodic behavior is due to the asynchronism ($2\gamma_2 - \gamma_1 - \gamma_3 \neq 0$) of the three supermodes. When this condition is met (it occurs at $\Delta n = -0.00023$), $P_{\text{out},1}$ and $P_{\text{out},3}$ do show periodic behaviors as shown in Fig. 4(a), where $L_C = 2\pi/(\gamma_1 - \gamma_3)$ is evaluated at that $\Delta n \neq 0$. However,

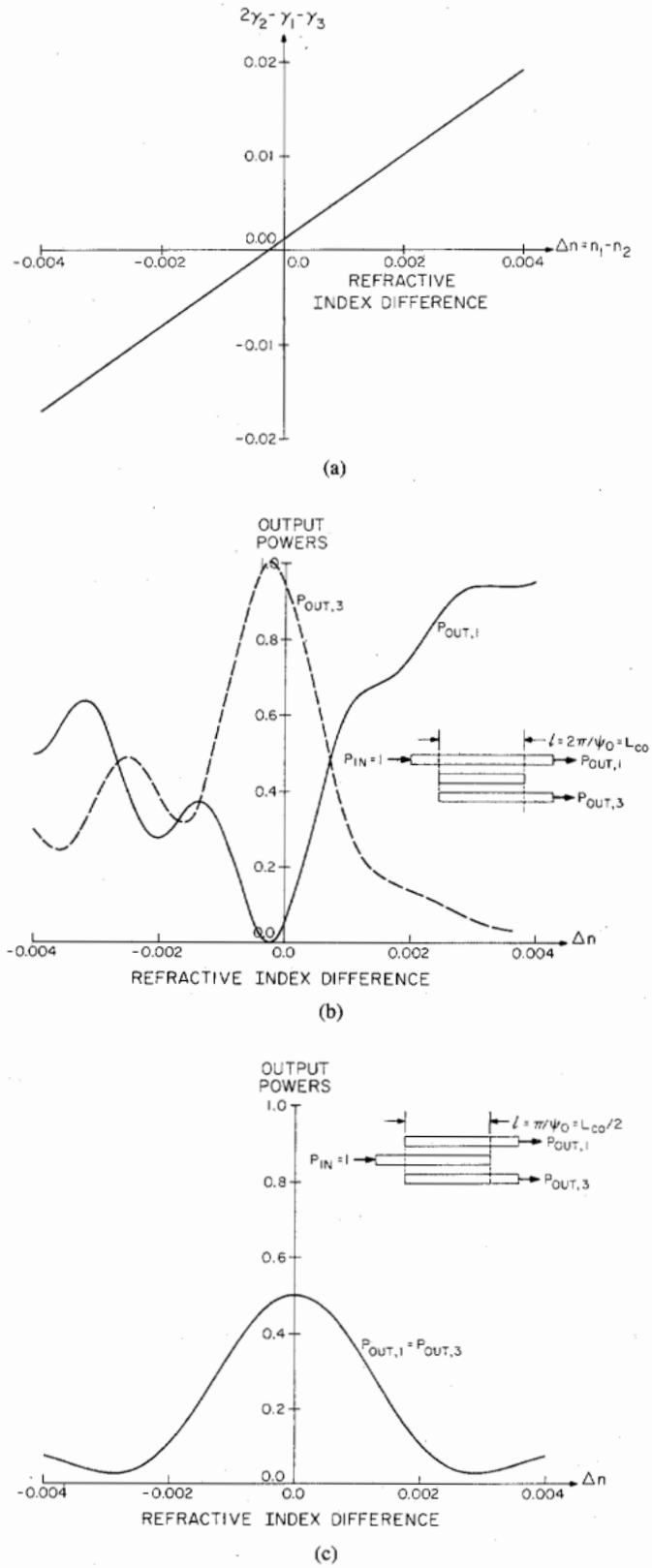

Fig. 2. (a) The asynchronism $2\gamma_2 - \gamma_1 - \gamma_3$ of three-coupled waveguides are plotted versus the refractive index difference $\Delta n = n_1 - n_2$, which is proportional to the applied voltage. The parameters are all similar to those in Fig. 1. $d_1 = d_2 = d_3 = 2$ μm. $t = 1.9$ μm, $\lambda = 1.06$ μm, $n_1 = n_3 = 2.2 + \Delta n/2$, $n_2 = 2.2 - \Delta n/2$. $L_{C0} = 0.8105$ mm. (b) The output powers $P_{\text{OUT},1}$ (solid curve) and $P_{\text{OUT},3}$ (dashed curve) are shown for the power transfer devices with input power $P_{\text{IN}} = 1$ in waveguide 1. (c) The output powers $P_{\text{OUT},1} = P_{\text{OUT},3}$ are plotted versus Δn when the three-waveguide coupler in (a) is used as a power divider.

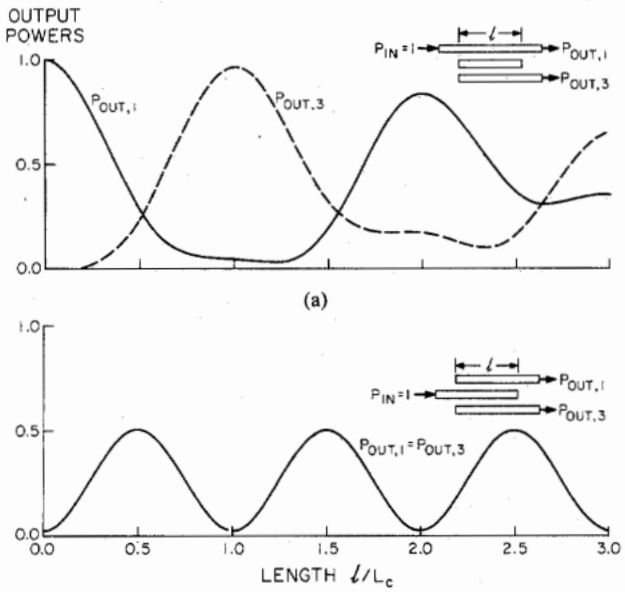

Fig. 3. (a) The output powers $P_{OUT,1}$ (solid curve) and $P_{OUT,3}$ (dashed curve) are plotted versus the coupling distance l normalized to L_C for a power transfer device. The same parameters from Fig. 2 are used except that Δn is fixed to be zero and l is varying. (b) The output powers $P_{OUT,1} = P_{OUT,3}$ are plotted versus the normalized distance l/L_C when the three coupled waveguides in Fig. 2(c) are used as power dividers. ($\Delta n = 0$, l is varying here.)

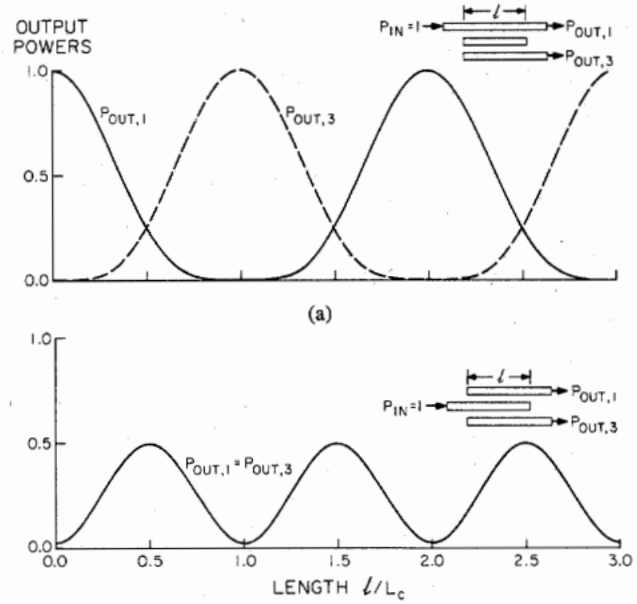

Fig. 4. (a) The output powers $P_{OUT,1}$ (solid curve) and $P_{OUT,3}$ (dashed curve) are plotted versus the normalized coupling distance l/L_C for the case $\Delta n = 0.00023$ where $2\gamma_2 - \gamma_1 - \gamma_3 = 0$. (b) Similar conditions hold as (a) except that the device is used as a power divider.

the output powers for the power dividers always show periodic functions because of the symmetry of the excitation and the waveguide structure (only two of the three supermodes, γ_1 and γ_3, are excited). It is easy to see from (35) that the output powers will be periodic functions of the distance l for both Fig. 3(b) ($2\gamma_2 - \gamma_1 - \gamma_3 \neq 0$) and Fig. 4(b) ($2\gamma_2 - \gamma_1 - \gamma_3 = 0$).

IV. Crosstalk Problems

Crosstalk problems have been investigated recently for two-coupled waveguides [18] and three-coupled waveguides [19] using either the conventional coupled-mode theory or direct numerical approach for the propagation constants. We apply the strongly coupled mode equations here to investigate the crosstalk problems.

A. Crosstalks in Two-Coupled Waveguides

In the design of two-coupled waveguides, one usually chooses the coupling length l such that

$$\psi l = n\pi/2, \qquad n = \text{odd integer} \tag{39}$$

and $b(l)$ is maximum, $a(l) = 0$ provided that $\Delta = 0$, i.e., two waveguides are identical. One finds immediately that the output power in waveguide b is maximum. However, the output power in waveguide a is not zero because there is still an overlap of fields between modes in waveguides a and b. This crosstalk power is easily obtained by setting $\delta = 0$ in (25) as a conservative estimation [18]

$$\text{Extinction ratio} = P_a(\delta = 0) = C_{12}C_{21} = \overline{C}_{12}^2 \tag{40}$$

since $C_{12} = C_{21}$ when two waveguides are identical. The formula (40) only provides a conservative estimation since it assumes waveguide a continues. In reality, guides a and b may start to separate at $z = l$ gradually. Thus, (40) is only an approximation [18].

This result showing that the crosstalk is proportional to the square of the overlap integral agrees with that obtained in [18]. However, our numerical calculations show that for two-coupled GaAs waveguides with the dimensions $d_a = d_b = 2$ μm, the edge-to-edge separation $t = 1.9$ μm, the refractive indexes $n_a = n_b = 3.44$, and the outside refractive index $n_0 = 3.436$, the crosstalk is -10 dB, which is close to -12.6 dB of [18] but not identical. We believe our number is more accurate since we have calculated the propagation constants β_1 and β_2 up to 7 digits (after the decimal point) of accuracy; the power conservation and the exact analytical relations are all checked so that the errors are always less than 10^{-7}. The studies of crosstalks in [18], [19] assume identical waveguides and the refractive indexes are fixed ($\Delta n = 0$). One finds using Fig. 1(d) that the crosstalk P_a can actually be given by (25). At $\Delta n \simeq -0.0002$, the extinction ratio goes to zero! Thus a very good extinction ratio can be obtained with a slight asymmetry introduced in the two waveguides with $\Delta n \neq 0$.

B. Crosstalks in Three-Coupled Waveguides

Three-coupled waveguides have been introduced to decrease the crosstalks when used as power transfer devices from one outer waveguide to another.

However, the synchronism condition

$$2\gamma_2 - \gamma_1 - \gamma_3 = 0$$

needs to be satisfied; otherwise, the crosstalks may be proportional to the overlap integrals C_{12} and C_{23} of the

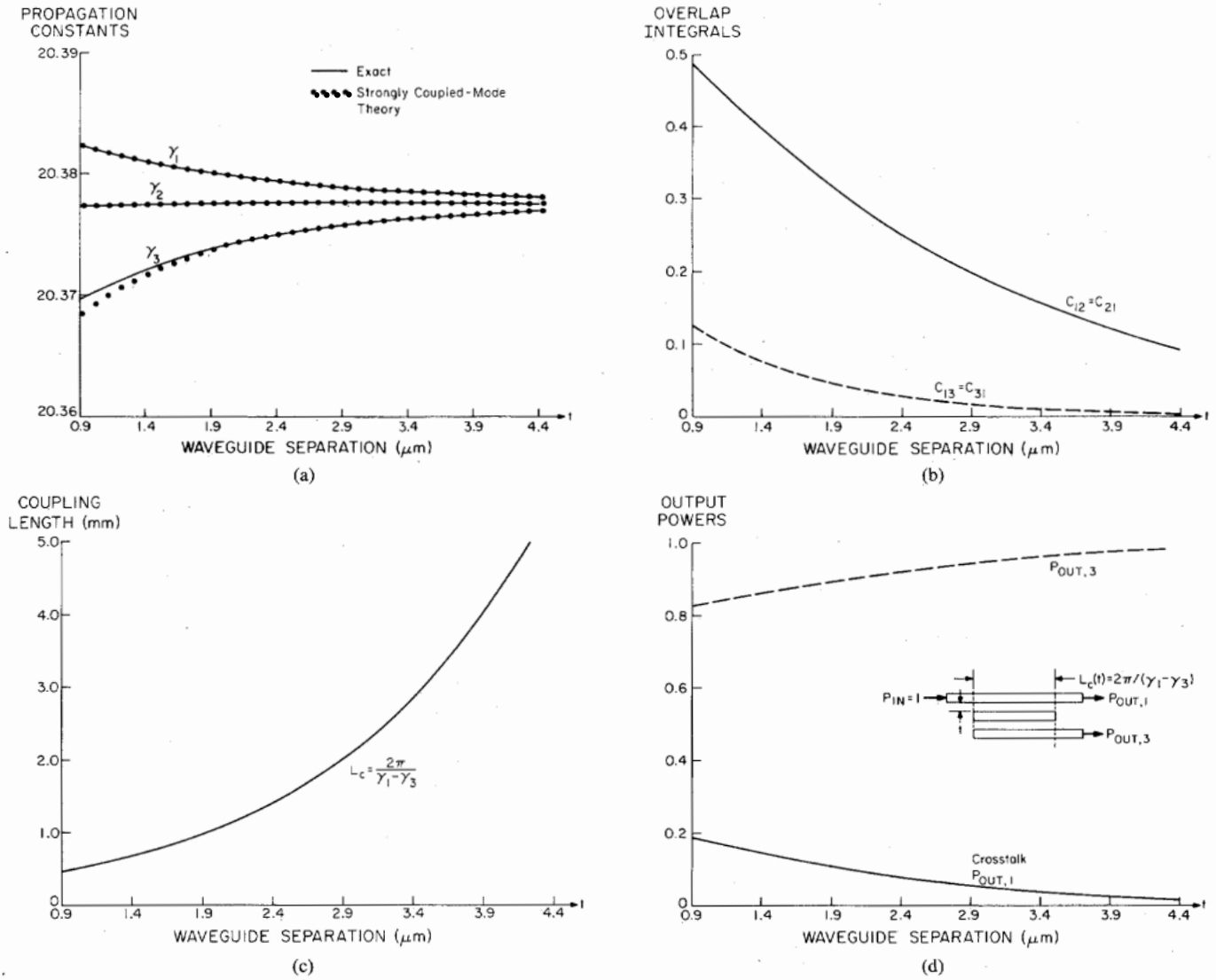

Fig. 5. (a) The propagation constants of the three supermodes using the strongly coupled-mode theory (dotted lines) are compared with the exact numerical calculations (solid lines). The waveguide edge-to-edge separation t is varied. The parameters are $d_1 = d_2 = d_3 = 2\ \mu$m, $n_1 = n_2 = n_3 = 3.44$, $n_0 = 3.436$. $\lambda = 1.06\ \mu$m. (b) The overlap integrals $C_{12}(= C_{21})$ and $C_{13}(= C_{31})$ are plotted versus the wavelength edge-to-edge separation t. (c) The coupling distance $L_C = 2\pi/(\gamma_1 - \gamma_3)$ is illustrated. (d) The output power $P_{\text{OUT},3}$ (dashed line) in the guide 3 and the extinction ratio $P_{\text{OUT},1}$ (solid line) due to crosstalk are shown.

two nearby modes instead of the two outer guided modes C_{13}. When used as power transfer devices, one chooses

$$l = 2\pi/(\gamma_1 - \gamma_3) = 2\pi/\psi \tag{41}$$

or an integral multiple of l such that $a_2(l) = 0$. We find the extinction ratio to be (using $\sin \psi l = 0$)

$$\text{Extinction ratio } (= P_{\text{out},1}) = \sin^2\left[\frac{2\gamma_2 - \gamma_1 - \gamma_3}{4} l\right] + C_{13}^2 \cos^2\left[\frac{2\gamma_2 - \gamma_1 - \gamma_3}{4} l\right]$$

$$= \sin^2\left[\frac{2\gamma_2 - \gamma_1 - \gamma_3}{2(\gamma_1 - \gamma_3)} \pi\right] + C_{13}^2 \cos^2\left[\frac{2\gamma_2 - \gamma_1 - \gamma_3}{2(\gamma_1 - \gamma_3)} \pi\right] \tag{42}$$

and similarly, the output power

$$P_{\text{out},3} = \cos^2\left[\frac{2\gamma_2 - \gamma_1 - \gamma_3}{2(\gamma_1 - \gamma_3)} \pi\right] + C_{13}^2 \sin^2\left[\frac{2\gamma_2 - \gamma_1 - \gamma_3}{2(\gamma_1 - \gamma_3)} \pi\right]. \tag{43}$$

This analytical result for crosstalks is useful since it explains clearly the following.

1) If the synchronism condition is met

$$2\gamma_2 - \gamma_1 - \gamma_3 = 0$$

$$\text{Extinction ratio} = C_{13}^2$$

which is expected.

2) If the synchronism condition is not met, the first term will contribute, and it will be proportional to the square of its argument if the synchronism condition is only approximately met. For this case, we show directly numerical results instead of using the approximate analysis in [19].

In Fig. 5(a)–(d), we illustrate the numerical results for a three-coupled waveguide used as a power transfer device. The waveguide widths are $d_1 = d_2 = d_3 = 2$ μm, the refractive indexes are $n_1 = n_2 = n_3 = 3.44$, and the outside refractive index $n_0 = 3.436$ [19]. The wavelength λ is 1.06 μm. The waveguides' edge-to-edge separations t are varied between 0.9 μm (near cutoff) to 4.4 μm. In Fig. 5(a), the propagation constants of the three supermodes using the strongly coupled-mode theory are plotted and compared with those calculated exactly from solving the multilayered (slab) structure numerically. One finds very good agreement. A small discrepancy occurs for γ_3 when that mode is close to cutoff near $t = 0.9$ μm. The overlap integrals C_{12} (solid curve) and C_{13} (dashed curve) are plotted in Fig. 5(b) where C_{12} is as large as 0.49, i.e., coupling is indeed very strong. ($C_{13} \simeq 0.125$ at $t = 0.9$ μm is also large). The coupling length $L_c = 2\pi/(\gamma_1 - \gamma_3)$ is plotted in Fig. 5(c) versus the waveguide separation t. One finds the extinction ratio $P_{\text{out},1}$ due to crosstalks as shown in Fig. 5(d) decays as the waveguide separation t is increased. This has been discussed in [19] for a fixed separation $t = 1.9$ μm using a different approach. Our result, at that separation, gives $P_{\text{out},1} = 0.1082 = -9.66$ dB which is actually higher than -12 dB given in [19] where the overlap integral between the two outer guides C_{13} ($= 0.0435$) has been ignored. The results here should be more accurate since the exact propagation constants γ_1, γ_2, and γ_3 at $t = 1.9$ μm are calculated accurately up to 7 digits after the decimal point and are also confirmed by the strongly coupled-mode theory. Taking the ratio of the extinction ratio $P_{\text{out},1}$ to the square of the overlap integral, C_{12}^2, one finds $P_{\text{out},1}/C_{12}^2 \simeq 0.78$ at $t = 0.9$ μm; 1.08 at $t = 1.9$ μm; 1.42 at $t = 2.9$ μm, and 1.75 at $t \simeq 3.9$ μm. Thus one may only say that the extinction ratio is roughly proportional to the square of the overlap integral C_{12}. The proportional constant estimated in [19] is $\approx \pi^2/2 = 4.9$ for weak coupling and $4.9/3 \simeq 1.63$ for strong coupling. The latter seems to agree better with our results since the coupling is pretty strong here. Thus the factor $\pi^2/2$ is not appropriate for the example presented in [19]. The strongly coupled-mode theory should be applied when numerical accuracy is essential.

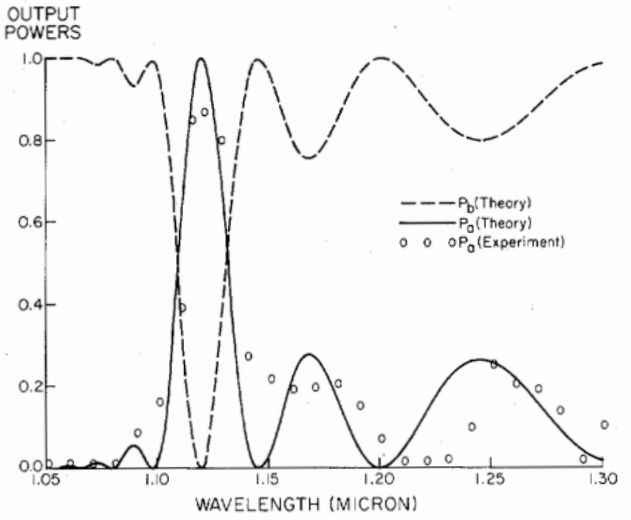

Fig. 6. The output powers of two coupled $In_xGa_{1-x}As_yP_{1-y}$–InP waveguides used as an optical wavelength filter. The input power is assumed to be 1 in waveguide b. The theoretical results for output powers at waveguide a, P_a (solid curve), at waveguide b, P_b (dashed curve), are compared with the experimental data (circles) for P_a.

V. Optical Wavelength Filters

Optical wavelength filters using waveguide couplers have been reported for Ti : $LiNbO_3$ and InGaAsP–InP materials. The $In_{1-x}Ga_xAs_yP_{1-y}$–InP material system is especially interesting because of its applications at 1.3 or 1.55 μm wavelength and its potential for optoelectronic integrated circuits. The experiment reported in [8] has two-coupled waveguides: one has a narrower guide width $d_a = 0.42$ μm, but a larger refractive index n_a (obtained following [21]) with $y_a = 0.127$; the other has the guide width $d_b = 0.91$ μm and $y_b = 0.078$ (n_b is also obtained following [21]). The Ga mole fraction x_a (or x_b) depends on the As mole fraction y_a (or y_b) for lattice matching [21]. The input power is assumed to be 1 in waveguide b. The results of a direct numerical approach have been shown in [8] and compared with the experimental data. We have applied the strongly coupled-mode theory using (25) and (26) (exchanging a and b since the input is in guide b instead of in a) and compared our theoretical results with the experimental results in Fig. 6. The agreement is very similar to that in [8]. The parameters reported in [8] used for the theoretical calculations are within the measurement accuracy. No detailed explanations are given for the small discrepancy between the results for the theory and the experiment. We think the possible reasons may be 1) there is still some difference between the theoretical model in [21] and the experimental values for the refractive index, and 2) the losses in the waveguides are not taken into account. However, the comparison shown in Fig. 6 does show very good results.

VI. Conclusions

A strongly coupled-mode theory [9]–[11], [13], [14] has been presented and combined with the theory of Marcatili [15] for the two-coupled waveguide case. The applica-

tions to two- and three-waveguide couplers, including power transfer devices and power dividers, have been investigated. This coupled-mode theory is applicable to very general cases for parallel dielectric waveguides with strong coupling and modes of general polarizations. It also accounts for the asymmetry of the waveguides and satisfies the energy conservation law and the reciprocity theorem self-consistently [13], [14]. The crosstalk problems in two- and three-coupled waveguides and their applications as optical wavelength filters have also been investigated and compared with the experimental data [8].

Appendix A

The Matrix Elements C_{pq}, $\overline{C}_{pq}$, K_{pq}, $\overline{K}_{pq}$ and the Field Expressions

1) Matrix Elements for the Overlap Integrals:

$$C_{pq} = \tfrac{1}{2} \int_{-\infty}^{\infty} \boldsymbol{E}_t^{(q)} \times \boldsymbol{H}_t^{(p)} \cdot \hat{z}\, dx\, dy \tag{A1}$$

$$\begin{aligned} \overline{C}_{pq} &= \tfrac{1}{2}(C_{pq} + C_{qp}) \\ &= \overline{C}_{qp}. \end{aligned} \tag{A2}$$

2) Matrix Elements for the Coupling Coefficients: "Conventional" coupling coefficients

$$\overline{K}_{pq} = \frac{\omega}{4} \int\int \Delta\epsilon^{(q)} [\boldsymbol{E}_t^{(p)} \cdot \boldsymbol{E}_t^{(q)} - E_z^{(p)} E_z^{(q)}]\, dx\, dy \tag{A3}$$

$$\Delta\epsilon^{(q)} = \epsilon(x, y) - \epsilon^{(q)}(x, y) \tag{A4}$$

where $\epsilon(x, y)$ is the permittivity function of the multiwaveguide system and $\epsilon^{(q)}(x, y)$ is the permittivity function of a single waveguide q.

New K_{pq} used in (4) of this paper [13], [14]:

$$K_{pq} = \frac{\omega}{4} \int\int \Delta\epsilon^{(q)} [\boldsymbol{E}_t^{(p)} \cdot \boldsymbol{E}_t^{(q)} - \frac{\epsilon^{(p)}}{\epsilon} E_z^{(p)} E_z^{(q)}]\, dx\, dy. \tag{A5}$$

3) The Field Expressions for the Supermode: The transverse components are

$$\boldsymbol{E}_t = \sum_p a_p(z)\, \boldsymbol{E}_t^{(p)}(x, y) \tag{A6}$$

$$\boldsymbol{H}_t = \sum_p a_p(z)\, \boldsymbol{H}_t^{(p)}(x, y). \tag{A7}$$

The longitudinal components are

$$E_z = \sum_p a_p(z) \frac{\epsilon^{(p)}}{\epsilon} E_z^{(p)}(x, y) \tag{A8}$$

$$H_z = \sum_p a_p(z)\, H_z^{(p)}(x, y). \tag{A9}$$

Appendix B

A Formal Treatment of Two-Coupled Waveguides for a Lossless System

The coupled-mode equations are assumed to be of the form in general:

$$\frac{d}{dz} a(z) = i\gamma_a a(z) + iK_{ab} b(z) \tag{B1}$$

$$\frac{d}{dz} b(z) = i\gamma_b b(z) + iK_{ba} a(z) \tag{B2}$$

where we have assumed for the transverse fields

$$\boldsymbol{E}_t = a(z)\, \boldsymbol{E}_t^{(a)} + b(z)\, \boldsymbol{E}_t^{(b)} \tag{B3}$$

$$\boldsymbol{H}_t = a(z)\, \boldsymbol{H}_t^{(a)} + b(z)\, \boldsymbol{H}_t^{(b)} \tag{B4}$$

and the transverse components $\boldsymbol{E}_t^{(a)}$, $\boldsymbol{E}_t^{(b)}$, $\boldsymbol{H}_t^{(a)}$ and $\boldsymbol{H}_t^{(b)}$ are all real. Thus, one finds that γ_a, γ_b, K_{ab}, and K_{ba} are all real. Power conservation leads to

$$\begin{aligned} 0 = \frac{d}{dz} P(z) &= \frac{d}{dz} \frac{1}{2} \operatorname{Re} \int\int \boldsymbol{E}_t \times \boldsymbol{H}_t^* \cdot \hat{z}\, dx\, dy \\ &= \frac{d}{dz} \operatorname{Re} [aa^* + ab^* \overline{\overline{C}}_{21} + ba^* \overline{\overline{C}}_{12}^* + bb^*] \\ &= \frac{d}{dz} [aa^* + (ab^* + ba^*)\, \bar{c} + bb^*] \\ &= ab^* i(\gamma_a \bar{c} - \gamma_b \bar{c} + K_{ba} - K_{ab}) \\ &\quad + ba^* i(\gamma_b \bar{c} - \gamma_a \bar{c} + K_{ab} - K_{ab}) \end{aligned} \tag{B5}$$

where we have used (B1), (B2), the fact that $\overline{\overline{C}}_{12}$, $\overline{\overline{C}}_{21}$ are real, and

$$\begin{aligned} \bar{c} &= \frac{\overline{\overline{C}}_{12} + \overline{\overline{C}}_{21}^*}{2} \\ &= \overline{C}_{12}. \end{aligned} \tag{B6}$$

Since both a and b are arbitrary, we conclude that the coefficients in front of ab^* and ba^* are zero and obtain

$$K_{ab} - K_{ba} = (\gamma_a - \gamma_b)\, \bar{c} \tag{B7}$$

which is the general lossless condition that the four parameters in the coupled-mode equations (B1) and (B2) must satisfy.

References

[1] H. Kogelnik, "Theory of dielectric waveguides," in *Integrated Optics*, T. Tamir, Ed. New York: Springer-Verlag, 1979, 2nd ed., ch. 2.

[2] A. Yariv, "Coupled-mode theory for guided-wave optics," *IEEE J. Quantum Electron.*, vol. QE-9, pp. 919–933, 1973.

[3] H. F. Taylor and A. Yariv, "Guided wave optics," *Proc. IEEE*, vol. 62, pp. 1044–1060, 1974.

[4] E. Kapon, J. Katz, and A. Yariv, "Supermode analysis of phase-locked arrays of semiconductor lasers," *Opt. Lett.*, vol. 9, pp. 125–127, 1984.

[5] A. Hardy and W. Streifer, "Analysis of phased array diode lasers," *Opt. Lett.*, vol. 10, pp. 335–337, 1985.

[6] R. C. Alferness and R. V. Schmidt, "Tunable optical waveguide directional coupler filter," *Appl. Phys. Lett.*, vol. 33, pp. 161–163, July 1978.
[7] R. C. Alferness and J. J. Veselka, "Tunable Ti:$LiNbO_3$ waveguide filter for long-wavelength (λ = 1.3–1.6 μm) multiplexing/demultiplexing," in *Tech. Dig. Conf. Lasers and Electrooptics*, Anaheim, CA, 1984, pp. 230–231.
[8] B. Broberg, B. S. Lindgren, M. Öberg, and H. Jiang, "A novel integrated optics wavelength filter in InGaAsP-InP," *J. Lightwave Technol.*, vol. LT-4, pp. 196–203, 1986.
[9] A. Hardy and W. Streifer, "Coupled mode theory of parallel waveguides," *J. Lightwave Technol.*, vol. LT-3, pp. 1135–1146, 1985.
[10] ——, "Coupled modes of multiwaveguide systems and phase arrays," *J. Lightwave Technol.*, vol. LT-4, pp. 90–99, 1986.
[11] ——, "Coupled mode solutions of multiwaveguide systems," *IEEE J. Quantum Electron.*, vol. QE-22, pp. 528–534, Apr. 1986.
[12] H. A. Haus, W. P. Huang, S. Kawakami, and N. A. Whitaker, "Coupled-mode theory of optical waveguides," *J. Lightwave Technol.*, vol. LT-5, pp. 16–23, 1987.
[13] S. L. Chuang, "A coupled-mode formulation by reciprocity and a variational principle," *J. Lightwave Technol.*, vol. LT-5, pp. 5–15, 1987.
[14] ——, "A coupled-mode theory for multiwaveguide systems satisfying the reciprocity theorem and power conservation," *J. Lightwave Technol.*, vol. LT-5, pp. 174–183, 1987.
[15] E. Marcatili, "Improved coupled-mode equations for dielectric guides," *IEEE J. Quantum Electron.*, vol. QE-22, pp. 988–993, June 1986.
[16] J. P. Donnelly, N. L. DeMeo, Jr., and G. A. Ferrante, "Three-guide optical couplers in GaAs," *J. Lightwave Technol.*, vol. LT-1, pp. 417–424, 1983.
[17] J. P. Donnelly, "Limitations on power-transfer efficiency in three-guide optical couplers," *IEEE J. Quantum Electron.*, vol. QE-22, pp. 610–616, May 1986.
[18] K. L. Chen and S. Wang, "Cross-talk problems in optical directional couplers," *Appl. Phys. Lett.*, vol. 44, pp. 166–168, 1984.
[19] ——, "The crosstalk in three-waveguide optical directional couplers," *IEEE J. Quantum Electron.*, vol. QE-22, pp. 1039–1041, July 1986.
[20] W. Streifer, M. Osinski, and A. Hardy, "Reformation of the coupled mode theory of multiwaveguide systems," *J. Lightwave Technol.*, vol. LT-5, pp. 1–4, 1987.
[21] B. Broberg and S. Lindgren, "Refractive index of $In_{1-x}Ga_xAs_yP_{1-y}$ layers and InP in the transparent wavelength region," *J. Appl. Phys.*, vol. 55, p. 3376–3381, 1984.

Shun-Lien Chuang (S'78–M'82) was born in Taiwan in 1954. He received the B.S. degree in electrical engineering from National Taiwan University in 1976, and the M.S., E.E., and Ph.D. degrees in electrical engineering from the Massachusetts Institute of Technology, Cambridge, in 1980, 1981, and 1983, respectively.

While in graduate school, he held research and teaching assistantships, and also served as a recitation instructor. He conducted research at Schlumberger-Doll Research in Ridgefield, CT, during the summers of 1981 and 1982, and also in 1983 as a member of the professional staff. He is now an Assistant Professor with the Department of Electrical and Computer Engineering, University of Illinois at Urbana-Champaign. He is conducting research in electromagnetics, integrated optics, and semiconductor optoelectronic devices. He teaches courses on electromagnetics, solid-state electronic devices, and has recently developed a new graduate course on integrated optics and optoelectronics.

Dr. Chuang is a member of the Optical Society of America, Sigma Xi, and the American Physical Society. He has been cited several times by the University of Illinois for Excellence in Teaching.